BIODIVERSITAS
Volume 26, Number 12, December 2025
Pages: 6523-6540

ISSN: 1412-033X
E-ISSN: 2085-4722
DOI: 10.13057/biodiv/d261249

Microhabitat diversity of ancient trees in Hyrcanian Old-Growth Forests, Iran

ZAHRA VEYSI[1], MOHSEN JAVANMIRI POUR[2,♥], VAHID ETEMAD[3]

[1]Graduate student, Forestry and Forest Economic Department, Natural Resources Faculty, College of Agriculture and Natural Resources, University of Tehran. Daneshkadeh Ave, Mesbah, Karaj 77871-31587, Alborz Province, Iran

[2]Assistance professor, Kermanshah Agricultural and Natural Resources Research and Education Center, Agricultural Research, Education and Extension Organization. Kermanshah, Keshavarz Blvd 67145-1661, Iran. Tel./fax.: +98-83-38358444, ♥email: mjavanmiri@ut.ac.ir

[3]Associate professor, Forestry and Forest Economic Department, Natural Resources Faculty, College of Agriculture and Natural Resources, University of Tehran. Daneshkadeh Ave, Mesbah, Karaj 77871-31587, Alborz Province, Iran

Manuscript received: 11 June 2025. Revision accepted: 29 December 2025.

Abstract. *Veysi Z, Pour MJ, Etemad V. 2025. Microhabitat diversity of ancient trees in Hyrcanian Old-Growth Forests, Iran. Biodiversitas 26: 6523-6540.* Old-growth forests play a critical role in maintaining biodiversity by supporting diverse Tree-related Microhabitats (TreMs), yet their distribution patterns in Iran's Hyrcanian Old-Growth Forests remain understudied. This study presents the first systematic assessment of TreMs in temperate old-growth forests of northern Iran, focusing on 60 ancient trees across four key species: Oriental beech (*Fagus orientalis*), velvet maple (*Acer velutinum*), alder (*Alnus subcordata*), and hornbeam (*Carpinus betulus*) in Kheyrud Forest. We identified and analyzed 12 distinct TreM types, including cavities, deadwood, and epiphytes, and evaluated their spatial distribution using GIS alongside environmental variables (elevation, slope, stand structure). Our results demonstrate that velvet maple and beech trees host the highest TreM richness, functioning as keystone structures for habitat heterogeneity. Notably, velvet maple (*A. velutinum*) showed strong associations with woodpecker cavities, reflecting species-specific microhabitat relationships. Statistical analyses revealed significant variation in TreM distribution across tree species and forest types, emphasizing the importance of preserving diverse tree assemblages to sustain microhabitat complexity. These findings provide actionable insights for conserving the Hyrcanian Old-Growth Forests, a UNESCO-listed biodiversity hotspot, and highlight the global relevance of protecting old-growth ecosystems for biodiversity resilience. By linking TreM patterns to forest structure and environmental gradients, this study establishes a foundation for evidence-based management strategies in temperate forests worldwide.

Keywords: Biodiversity, cavity, ecological functions, structural complexity, woodpecker

INTRODUCTION

Old-growth forests are among the most structurally and biologically complex terrestrial ecosystems, shaped over centuries through natural processes of disturbance, succession, and species interactions. These ecosystems are central to ecological theory regarding habitat heterogeneity and biodiversity, as they exemplify how complex physical structures generate diverse ecological niches that support highly specialized species assemblages. The habitat heterogeneity hypothesis posits that structurally diverse environments promote species coexistence by increasing resource availability and niche differentiation (MacArthur and MacArthur 1961). In this context, old-growth forests function as keystone ecosystems, supporting exceptional levels of biodiversity, carbon sequestration, and ecosystem stability (Gilhen-Baker et al. 2022).

A defining feature of old-growth forests is their structural complexity, including multilayered canopies, varied tree diameters, large deadwood volumes, and the presence of veteran trees bearing unique features such as cavities, bark fissures, and epiphytic growth (Finsinger et al. 2022). These features generate Tree-related Microhabitats (TreMs), small-scale structures that support distinct biotic communities. Such microhabitats are critical for organisms like saproxylic fungi, cavity-nesting birds, lichens, and invertebrates, many of which are highly specialized and sensitive to forest disturbance (Asbeck et al. 2021; Przepióra and Ciach 2022). As ecological theory suggests, these microhabitats enhance functional diversity, stabilize food webs, and increase forest resilience to environmental change (Larrieu et al. 2018; Bütler et al. 2021).

Among the world's remaining old-growth ecosystems, the Hyrcanian Old-Growth Forests along the southern Caspian Sea coast represent a globally significant temperate rainforest. With a lineage stretching back to the Tertiary period, these forests contain a unique mixture of relict and endemic species, many of which persisted in this Pleistocene refugium while disappearing elsewhere (Alavi et al. 2020; Hafizy and Goring 2021; Ramezani et al. 2023). Dominated by species such as *Fagus orientalis*, *Carpinus betulus*, and *Quercus castaneifolia*, mature Hyrcanian stands develop intricate structures comparable to their European counterparts, yet remain relatively understudied with respect to microhabitat dynamics (Rahmani and Bayat 2023).

Microhabitats, ranging from tree cavities and decaying wood to epiphytic mats and bark features, represent key ecological substrates that maintain biodiversity and

ecological processes in forests (Larrieu and Cateau 2016; Winter et al. 2022). Their occurrence is influenced by forest composition, stand age, environmental gradients, and human intervention. In managed forests, selective logging and removal of old trees reduce microhabitat availability and disrupt ecological continuity, whereas protected old-growth stands retain higher microhabitat abundance and diversity (Paillet et al. 2010; Marthy and Gorska 2024; Wirth et al. 2025).

Comparative studies across Europe and the Mediterranean reveal strong biogeographic and structural influences on microhabitat formation. For example, eastern European beech forests are rich in woodpecker cavities, while Mediterranean oak stands show greater epiphyte and deadwood diversity (Regnery et al. 2013; Haghighatdoust and Waez-Mousavi 2021; Winter et al. 2022). Recent research in Hyrcanian Old-Growth Forests suggests that certain features like root cavities and hollow bases dominate microhabitat types, yet little is known about how these vary by forest type or tree species (Javanmiri and Etemad 2024).

Globally, the abundance and richness of microhabitats peak in tropical forests, though old-growth temperate systems also play a critical role, particularly in supporting rare taxa dependent on large-diameter, senescent trees (Augustin et al. 2021; Nuber et al. 2024; Spinu et al. 2024). Forest management intensity has been shown to be a primary driver of microhabitat loss, with studies highlighting the conservation value of practices like habitat tree retention, natural regeneration, and deadwood preservation (Ranius et al. 2019; Asbeck et al. 2021; Maxence et al. 2021). Despite growing recognition of microhabitats in forest conservation, key gaps remain, particularly in non-European temperate forests. In the Hyrcanian region, where conservation concerns are mounting due to fragmentation and unsustainable land use, understanding how forest type and structural attributes influence microhabitat provision is urgently needed.

Given that TreM formation depends on species-specific traits (e.g., bark properties, decay rates) and environmental gradients (Paillet et al. 2010), we hypothesized that: (i) TreM diversity would vary significantly among tree species due to differences in bark properties and decay rates; (ii) Spatial patterns would correlate with forest structure and topography (elevation, slope). Objectives: (i) Quantify TreM diversity and abundance across four key tree species (*F. orientalis*, *Acer velutinum*, *Alnus subcordata*, *C. betulus*); (ii) Assess TreM spatial distribution using Geographic Information System (GIS) and environmental variables; (iii) Identify species-specific TreM associations (e.g., woodpecker cavities in *A. velutinum*). By addressing these gaps, this study provides the first systematic TreM assessment in the Hyrcanian Old-Growth Forests, informing conservation strategies for this globally significant biome and contributing to broader understanding of temperate old-growth ecology.

MATERIALS AND METHODS

Site description

The Educational and Research Forest of the Faculty of Natural Resources at the University of Tehran, commonly known as Kheyrud Forest, constitutes a vital ecological reserve within the Hyrcanian-Caspian Forest ecoregion of northern Iran (51°33'12"-51°39'56"E, 36°32'08"-36°45'05"N). This old-growth temperate forest, located 7 km east of Nowshahr in Mazandaran Province, Iran represents one of the most biologically significant remnants of the Pleistocene-relict Hyrcanian Old-Growth Forests, harboring exceptional biodiversity with numerous endemic species (Figure 1). The forest's complex ecosystem structure, characterized by ancient tree specimens, diverse microhabitats, and a multi-layered canopy, serves critical ecological functions including carbon sequestration and climate regulation.

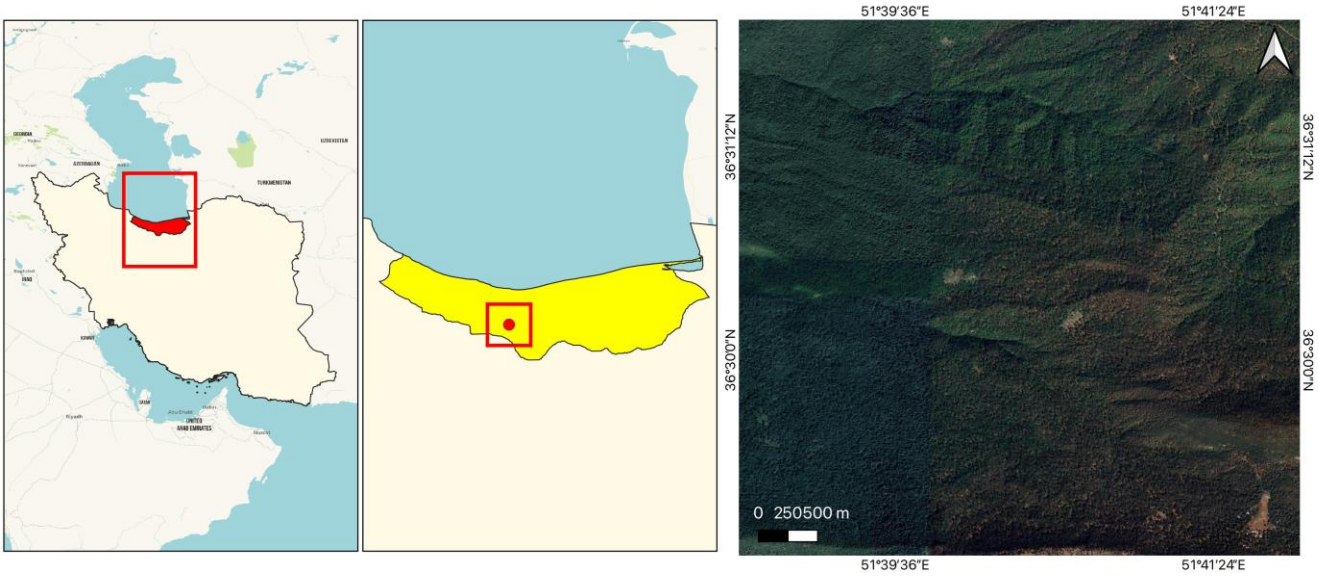

Figure 1. Study area location within the Hyrcanian Old-Growth Forests, Iran

Our study focuses on the Baharbon District (District 6), a 1,550-hectare area ranging from 1,000-2,200 m elevation that exemplifies the forest's vegetation zonation, bounded by Chelir Forest (north), Domain 46 (east), Hashtadtan ridge (south), and Kolyak River (west). The district contains characteristic forest associations including pure Oriental beech (*F. orientalis*), beech-hornbeam (*F. orientalis*-*C. betulus*), alder-velvet maple (*Alnus glutinosa*-*A. velutinum*), and other mixed stands, with companion species such as chestnut-leaved oak (*Q. castaneifolia*) and Caucasian lime (*Tilia begonifolia*). Despite its ecological importance as both a biodiversity hotspot and carbon sink, the forest faces mounting anthropogenic pressures including unsustainable logging practices and climate change impacts, underscoring the urgent need for research-informed conservation strategies.

Data collection

This study employed an integrated methodological framework that combined systematic field surveys with geospatial analysis to assess the distribution of ancient trees and the availability of microhabitats across late-successional Hyrcanian Old-Growth Forests in the Baharbon district. The study area was initially delineated using a 1:10,000-scale topographic map alongside a region-specific forest typology map, enabling precise identification of stand boundaries and preliminary vegetation mapping. Forest classification followed a multi-criteria approach, incorporating stand structural parameters, such as basal area, tree density, and canopy cover, as well as species composition and key physiographic factors, including elevation, slope, and aspect.

A hierarchical nomenclature system was applied to define forest types (Table 1). Pure stands were identified as those dominated (>90%) by a single species. Two-species types featured a primary species with 50-90% dominance and a tertiary species contributing less than 10%, with dominant species connected by an en dash (e.g., *F. orientalis*-*C. betulus*). Mixed stands lacked a single dominant species, with all species below 50% dominance and listed using commas. Three-species types were defined by the presence of three species each contributing more than 10% but none exceeding 50%. Main types were characterized by one or two species exceeding 50% combined abundance, whereas subtypes showed no such dominance, in accordance with regional phytosociological standards (Javanmiri et al. 2022).

Field data were collected using fixed-area plots (e.g., 500 m²), within which tree species identity, Diameter at Breast Height (DBH), tree height, estimated age (from increment coring in a subsample), and the presence of microhabitats (e.g., cavities, dead branches, epiphytic mats) were recorded. All plots were georeferenced using sub-meter accuracy GPS units, and standardized data collection protocols were applied to ensure consistency across survey teams.

Geospatial analyses were performed using ArcGIS Pro, employing overlay and spatial query functions to integrate forest typology and physiographic data with field observations. This approach enabled precise mapping and structural characterization of forest stands and veteran trees. The integration of spatial and ecological data supported robust, replicable identification of forest types and microhabitat-bearing trees, providing a sound basis for ecological interpretation aligned with regional vegetation classification and conservation planning frameworks.

This study utilized systematic field surveys conducted along 100-meter-wide transects within each delineated forest type to document the occurrence of ancient trees. Following standardized protocols adapted from regional methodologies (Azaryan et al. 2015), the geographic coordinates and dendrometric attributes of all encountered ancient trees were precisely recorded. Species-specific diameter thresholds, calibrated for local ecological conditions, were used to classify trees as ancient: *Fagus orientalis* (beech), *A. subcordata* (alder), *A. velutinum* (velvet maple), and *Acer pseudoplatanus* were designated as ancient at DBH ≥1.5 meters, while *C. betulus* (hornbeam) was classified as ancient at DBH ≥2 meters. The classification of trees as ancient uses species-specific DBH thresholds that reflect their unique growth patterns and longevity. For example, European beech (1.5 m DBH) reaches ancient status at smaller diameters than hornbeam (2+ m) due to its slower growth and shorter lifespan. Slow-growing, long-lived species like yew qualify at 2 m despite their extreme age, while dense hardwoods like oak require larger sizes (2.5-3 m) due to their decay resistance.

To maximize detection of veteran trees across heterogeneous terrain, a randomized, non-plot-based sampling approach was employed. A total of 60 ancient trees were recorded, reflecting the compositional structure of the stands: 28 beeches, 24 velvet maples, 6 alders, 1 hornbeam, and 1 chestnut-leaved oak (*Q. castaneifolia*), highlighting the ecological dominance of beech and velvet maple in these late-successional systems.

Table 1. Forest type classification system based on dominant tree species composition

Forest type	Species	Mixture of trees		
		First species	Second species	Third species
Main	beech	<90%	-	-
	Beech-Hornbeam	50%-90%	<50%	-
	beech, Hornbeam	>50%	>50%	-
Subordinate	beech-hornbeam with alder	50%-90%	<50%	<10%
	beech, hornbeam with velvet maple	<50%	>50%	<10%

The selection of 60 trees is justified by statistical, ecological, and practical factors. For quantitative studies, this sample size provides sufficient power (≥80%) to detect moderate effects (Cohen's d: 0.5) at α: 0.05 when comparing groups. In ecological research, 60 trees ensure thematic saturation, capturing dominant trends without excessive redundancy. The number balances representativeness and feasibility, aligning with standard guidelines (30-60 samples per stratum) while accommodating fieldwork constraints. This approach ensures robust, reliable results without impractical resource demands.

For each tree, detailed dendrometric measurements, including DBH, total height, crown architecture, and trunk condition, were obtained. In parallel, associated tree-related microhabitats were documented based on visible morphological features, resulting in the identification of twelve distinct types: woodpecker cavities, main trunk cavities, bark fissures, stem galls, natural nests, microsoils, fungal fruiting bodies, and multiple cavity forms in stumps or root bases.

Microhabitat distribution exhibited marked species-specific trends, with woodpecker cavities predominantly observed in thick-barked sycamores and stump cavities more frequently associated with mature beeches. All data were georeferenced and integrated into a Geographic Information System (GIS) framework. Spatial analyses incorporated key environmental variables, including elevation, slope, and aspect, to evaluate patterns of ancient tree distribution and microhabitat variability (Table 2; Figure 2). This spatially grounded approach provided a robust foundation for interpreting ecological processes shaping the structure and habitat value of late-successional Hyrcanian Old-Growth Forests.

To effectively analyze tree ecosystems using GIS, it is essential to incorporate multiple environmental variables that collectively influence growth and distribution. Beyond basic topographic features like elevation and slope, critical factors include soil characteristics (moisture content, pH, and texture), microclimate conditions (canopy cover density, understory light availability, and temperature gradients), and biotic interactions (competition indices and vegetation stress indicators). These variables, derived from high-resolution datasets such as LiDAR and SoilGrids, enable precise habitat modeling and species-specific assessments, for instance, evaluating drought tolerance in beech or light requirements for hornbeam regeneration. By integrating these multidimensional parameters, GIS analysis provides a robust foundation for ecological research, conservation planning, and sustainable forest management. The classification of TreMs in this study adhered to the standardized framework developed by Stokland et al. (2012), which categorizes trees into four hierarchical size classes based on the abundance and complexity of their associated microhabitats.

The smallest class comprised trees bearing 1 to 3 simple microhabitats, such as minor bark fissures or small stump cavities. These features typically indicate early-stage habitat development and are commonly found on younger trees or species exhibiting slower structural degradation and higher resistance to environmental stress.

The intermediate class included trees with 4 to 6 microhabitats, characterized by more complex structures such as woodpecker cavities, stem galls, and trunk fungi. These features reflect trees in mid-successional phases, possessing moderate structural complexity.

Trees in the large class, with 7 to 9 microhabitats, exhibited well-developed formations including deep trunk cavities, substantial natural nests, and stratified microsoils. Such trees were generally mature individuals (DBH ≥1.5 m), particularly Oriental beech (*F. orientalis*) and velvet maple (*A. velutinum*), species known for thick bark and high decay potential.

The very large class, representing the highest ecological significance, encompassed trees supporting more than 10 complex microhabitats. These trees often featured rare and diverse structures, such as multiple nesting cavities, varied fungal fruiting bodies, and multilayered microsoils. As senescent individuals, they act as keystone ecological structures and biodiversity hotspots, providing critical habitat resources rarely found in managed or younger forests.

Table 2. Classification system for tree microhabitats (adapted from Bütler et al. (2021)

Row	Microhabitat type	Abbreviation	Definition
1	Wood pecker cavity	WPC	Holes created by woodpeckers (hole diameter less than 10 cm)
2	Trunk cavity	TC	Holes on the main trunk (at least 10 cm in diameter)
3	Branch hole	BH	Holes with a minimum diameter of 5 cm on the main branches
4	Trunk base rot hole	TB	Holes on the base with a minimum diameter of 15 cm with water accumulation
5	Crack in the bark	CB	Trees with decay and cracks on the bark with a minimum area of 25 cm
6	Canker	CA	Observation of unusual extra growth with a minimum diameter of 20 cm
7	Nest	NE	The presence of bird nests or some vertebrates
8	Microsoil	MS	Accumulation of soil on the cracks of trunk bark or thick branches
9	Buttress root concavity	BRC	Holes on the buttress with a maximum diameter of 15 cm
10	Dead wood	DW	The presence of rotten or completely dried branches in the crown or main branches of the tree
11	Stem fungi	SF	Macroscopic fungi grown on the main trunk of the tree with a minimum size of 5 cm
12	Crack in the stem	CS	The presence of a crack on the main trunk with a length of at least 30 cm, a width of one cm and a depth of 10 cm

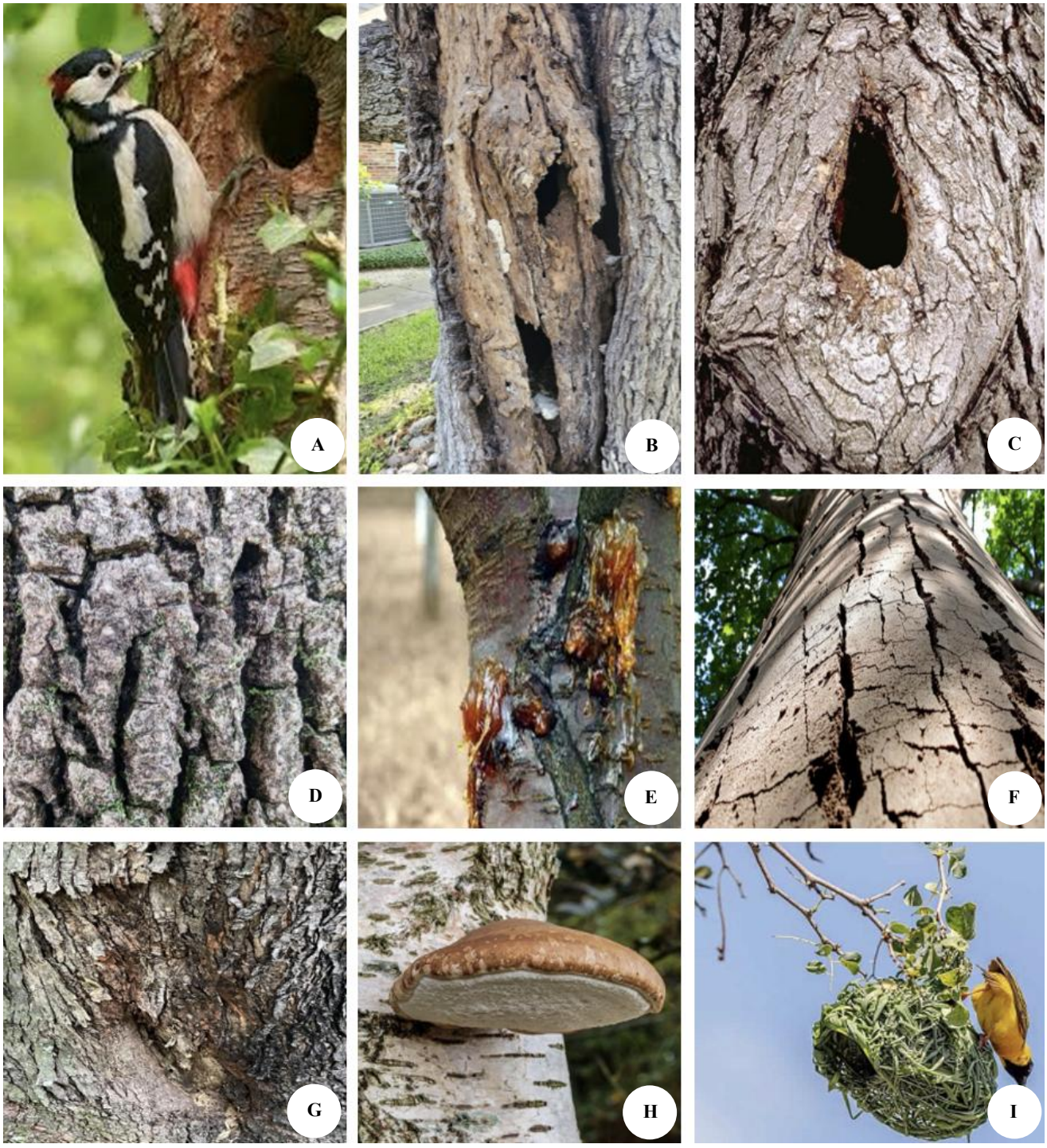

Figure 2. Diagnostic tree cavity types and habitat structures observed in the study area. A-I: Representative examples of key microhabitats: A. Primary cavity excavated by great spotted woodpecker (*Dendrocopos major*), showing characteristic 5-7 cm circular entrance; B. Branch hole formed by limb loss, with visible heartwood decay; C. Trunk cavity with multiple entrance holes indicating successive use; D. Bark fissure (>2 cm depth) providing arthropod refugia; E. Bacterial canker (*Pseudomonas syringae*) with resin bleeding; F. Stem crack extending >50 cm vertically; G. Microsoil accumulation in bark pockets (>200 cm³); H. Bracket fungi (*Fomes fomentarius*) on decayed sapwood; I. Passerine nest constructed in lateral cavity. Scale bars: 5 cm (A-C, F, I), 10 cm (D, E, G, H)

This hierarchical TreM classification offers a robust framework for assessing habitat quality and conservation value across forest developmental stages and is particularly effective in identifying legacy trees essential to the structural and ecological integrity of old-growth forests.

Forest ecosystems generally follow predictable successional trajectories, progressing from initiation and establishment through maturity and ultimately entering the senescence phase (Palik et al. 2021). The senescence stage is especially significant in temperate forests, marking a

period of marked physiological decline and structural transformation that creates ecologically valuable conditions. As trees age, they undergo biological degradation manifested by crown dieback, progressive branch mortality, and internal trunk decay. These processes often result from reduced photosynthetic capacity and diminished defenses against biotic agents such as wood-boring insects and pathogenic fungi.

Concurrently, natural disturbances-including windthrow, snow loading, and lightning strikes-become more frequent or severe during senescence, generating canopy gaps that initiate localized regeneration dynamics. These gaps modify microclimatic conditions, increase structural heterogeneity, and facilitate species turnover by allowing the establishment of shade-intolerant or mid-successional species.

At the stand level, the senescence phase produces characteristic spatial and structural configurations, ranging from irregular single-cohort structures with diverse tree diameters and spacing to pseudo-even-aged stands with relatively uniform canopy layers. These emergent patterns, shaped by both autogenic decline and external disturbances, contribute substantially to habitat complexity and ecological resilience, highlighting the critical conservation value of late-successional and old-growth forests.

In the Hyrcanian Old-Growth Forests of northern Iran, the old-growth phase in unmanaged natural stands typically spans 200 to 250 years, allowing for the full development of late-successional structural and ecological characteristics. In contrast, managed forests often exhibit shortened developmental trajectories due to silvicultural interventions that modify natural stand dynamics, including alterations in species composition, canopy structure, and disturbance regimes. The extended senescence period in natural stands fosters the accumulation of structural complexity, such as the formation of diverse tree-related microhabitats and the persistence of slow, continuous nutrient cycling processes. These structural and functional transformations are essential for sustaining the high biodiversity levels commonly associated with old-growth ecosystems. Consequently, senescent stands serve as critical biological reservoirs and play a pivotal role in bolstering forest ecosystem resilience in the face of changing environmental conditions.

In this study, biodiversity indices were calculated to quantitatively assess the biological variability and structural complexity of the ecosystem. These indices combine two fundamental components: species richness, the total number of species present, and species evenness, which reflects the relative abundance distribution among species. By integrating both aspects, biodiversity indices offer a nuanced and ecologically meaningful measure of diversity. For example, an ecosystem with high species richness but dominated by a few taxa exhibits lower overall diversity than one with a more balanced species distribution.

Among the widely used metrics, the Shannon-Wiener Index (H') incorporates species proportional abundances via a logarithmic function, providing a single composite value that captures both richness and evenness. This index enables meaningful comparisons across forest types, successional stages, or management regimes. Additionally, it supports long-term biodiversity monitoring and conservation planning by highlighting areas of high ecological integrity or vulnerability (Krebs 1999).

To evaluate biodiversity by incorporating both species richness and relative abundance, the Shannon-Wiener diversity index (H′) was calculated using the formula (1).

$$H' = -\sum_{i=1}^{S} p_i \ln p_i \quad [1]$$

Where p_i is the proportion of individuals belonging to species i and S is the total number of species. This index accounts for both the number of species and the evenness of their distribution within the community. Higher values of H′ indicate greater diversity and community stability, while lower values reflect skewed dominance by one or a few species. The Shannon-Wiener index was chosen for its sensitivity to both rare and common species and its widespread acceptance as a robust indicator of ecological complexity.

To quantify species evenness, we used the Pielou-modified evenness formula:

$$\text{Evenness} = e^{H'}/S \quad [2]$$

Where, H' is the Shannon-Wiener diversity index and S is species richness (the total number of species observed). This index scales evenness between 0 and 1, with values closer to 1 indicating a more uniform distribution of individuals among species. The exponential transformation of H' (i.e., e^H') represents the effective number of equally common species, aligning with the concept of Hill numbers, and dividing by species richness provides a relative measure of how evenly individuals are distributed. This approach allows for direct comparison of evenness across forest types and contributes to a more comprehensive understanding of biodiversity patterns.

To assess biodiversity under conditions where complete or near-complete enumeration was achieved, the Brillouin diversity index (H_B) was also calculated. Unlike the Shannon-Wiener index, which assumes random sampling, the Brillouin index is appropriate when the full composition of a community is known or when sampling is exhaustive.

$$H_B = \frac{\ln N! - \sum \ln n_i!}{N} \quad [3]$$

Where, N is the total number of individuals and n_i is the number of individuals of the ith species. The Brillouin index provides a robust measure of diversity by incorporating both species richness and abundance distribution, and it is less sensitive to sampling assumptions. Its inclusion enhances the reliability of diversity comparisons across forest types and management regimes.

To quantify species diversity with a focus on both richness and dominance, Simpson's Diversity Index in its complementary form (1-D) was calculated using the formula:

$$1 - D = 1 - \sum_{i=1}^{S} \left(\frac{n_i}{N}\right)^2 \quad [4]$$

Where, *n_i* is the number of individuals of species *i*, *N* is the total number of individuals in the sample, and *S* is species richness. This index estimates the probability that two individuals randomly selected from a community belong to different species. Higher values of (1-D) indicate greater biodiversity, with more balanced species representation. Simpson's index is particularly robust to sample size variation and less sensitive to rare species, making it a useful complement to other diversity metrics like Shannon and Margalef.

To evaluate species richness while accounting for differences in sample size, Menhinick's Index was calculated using the formula:

$$D_{Mn} = \frac{S}{\sqrt{N}} \quad [5]$$

Where, S represents the total number of species and N the total number of individuals recorded in each sample. This index provides a standardized richness metric that enables comparison across forest types or management regimes with varying sampling intensities. Its application is particularly valuable in field-based ecological studies where total individual counts differ among survey units.

To further quantify species richness in a standardized manner, Margalef's Diversity Index (D_{Mg}) was calculated using the formula:

$$D_{Mg} = \frac{S - 1}{\ln N} \quad [6]$$

Where, S is the number of species and N is the total number of individuals recorded. This index accounts for sampling effort by incorporating the natural logarithm of sample size and is particularly effective for comparing species richness across forest types with differing population densities. Its inclusion complements other diversity metrics by emphasizing the richness component independent of evenness.

To assess the evenness component of biodiversity, Pielou's Equitability Index (J) was calculated using the formula:

$$J = \frac{H'}{\ln S} \quad [7]$$

Where, H′ is the Shannon-Wiener diversity index and S is species richness. This index quantifies the degree to which individuals are evenly distributed among the species present. Values close to 1 indicate that species are nearly equally abundant, whereas lower values suggest dominance by one or a few species. The equitability index complements other diversity measures by highlighting structural imbalances in species composition and helps distinguish between communities with similar richness but different dominance structures.

To complement non-parametric diversity indices, Fisher's Alpha diversity index (α) was calculated based on the logarithmic series model, using the formula:

$$S = \alpha \cdot \ln\left(1 + \frac{N}{\alpha}\right) \quad [8]$$

Where, S is the number of species and N is the total number of individuals in the sample. Unlike other indices, Fisher's Alpha is relatively robust to variations in sample size and is particularly appropriate for datasets with a high proportion of rare species. The index was computed numerically using statistical software, allowing for reliable comparisons of diversity across forest types with differing levels of species richness and abundance.

To assess species dominance within the forest community, the Berger-Parker dominance index (d) was calculated using the formula:

$$d = \frac{N_{\max}}{N} \quad [9]$$

Where, N_{max} is the number of individuals in the most abundant species and N is the total number of individuals observed. This index provides a straightforward measure of dominance, with higher values indicating increased skew in species abundance. For comparative purposes, we also report the reciprocal form (1/d), which allows interpretation as a diversity metric, higher values reflect a more balanced community structure. The Berger-Parker index is especially useful for detecting shifts in community dominance due to disturbance, succession, or management interventions.

Data analysis

Following field data collection, all datasets were systematically organized and subjected to preliminary quality control and validation using Microsoft Excel (Office 365). Prior to conducting inferential analyses, statistical assumptions were rigorously evaluated to determine the appropriateness of parametric methods. Levene's test (α: 0.05) was used to assess the homogeneity of variances across groups, while the Kolmogorov-Smirnov test with Lilliefors correction verified the normality of data distributions. Upon confirmation of these assumptions, a one-way Analysis of Variance (ANOVA) followed by Tukey's HSD post-hoc test was applied to detect significant differences in microhabitat distribution among forest sites ($p<0.05$). For targeted pairwise comparisons between specific forest types or tree species, independent samples t-tests with Bonferroni correction were performed to control for Type I error. All statistical analyses were conducted using IBM SPSS Statistics (Version 26.0, Armonk, NY), selected for its robust data handling

capabilities, advanced modeling tools (e.g., GLMs, mixed-effects models), and reproducibility features. Non-parametric tests (Kruskal-Wallis/Mann-Whitney U) were employed where data violated parametric assumptions (Shapiro-Wilk $p<0.05$; heteroscedasticity in Levene's test) or for ordinal/interval variables (e.g., canopy cover classes). Additionally, PAST software was employed to analyze biodiversity indices. This analytical framework ensured methodological rigor and robustness in testing hypotheses related to microhabitat distribution patterns within old-growth forest ecosystems.

RESULTS AND DISCUSSION

Type of Beech exhibits a pronounced peak in the mid-range diameter classes, specifically between 170 cm and 195 cm, followed by a sharp decline in larger classes. Notably, there are no beech trees in the smallest (150 cm) or largest (290-295 cm) diameter classes. In contrast, Type of Other displays a more irregular and sporadic distribution across diameter classes. While there are isolated peaks at 170 cm, 180 cm, and 245 cm, many classes, such as 155-165 cm, 215-220 cm, and 265 cm, show minimal or no representation. The Sum of both types reinforces the dominance of beech in the mid-size classes, with the combined frequencies closely mirroring the beech distribution (Figure 3).

The Table 3, presents a comparative analysis of biodiversity indices for Type of Beech and Type of Others, revealing nuanced differences in species diversity, evenness, and dominance. Beech-dominated stands exhibited marginally higher diversity than mixed stands across multiple metrics, including Shannon entropy (H':3.291 vs 3.251) and evenness (0.8959 vs 0.8608), though mixed stands showed greater richness (Margalef: 4.093 vs 4.008; Fisher's α: 5.586 vs 5.402). The Berger-Parker index confirmed beech's dominance (0.086 vs 0.098), while Simpson (1-D: 0.958 vs 0.9551) and Brillouin (3.234 vs 3.187) values showed consistent but non-significant trends (paired t-test $p>0.05$ for all comparisons).

Type of oriental beech

Our comparative analysis of microhabitat distribution among velvet maple (*A. velutinum*), alder (*A. subcordata*), and beech (*F. orientalis*) revealed significant interspecific variation in both frequency and composition of microhabitats ($p<0.05$, ANOVA). The data demonstrate a clear hierarchy in microhabitat abundance, with velvet maple emerging as the most structurally complex species, exhibiting particularly high frequencies of trunk holes (n: 158±12.3) and woodpecker cavities (n: 152±9.8) per surveyed tree. These values significantly exceeded ($p<0.01$, Tukey HSD) those observed in other species.

Table 3. Comparative biodiversity metrics across forest types

Types	Simpson (1-D)	Shannon (H)	Evenness (e^H/S)	Brillouin	Menhinick	Margalef	Equitability J	Fisher alpha	Berger-Parker
Type of beech	0.958	3.291	0.8959	3.234	0.805	4.008	0.9677	5.402	0.086
Type of others	0.9551	3.251	0.8608	3.187	0.8678	4.093	0.9559	5.586	0.098

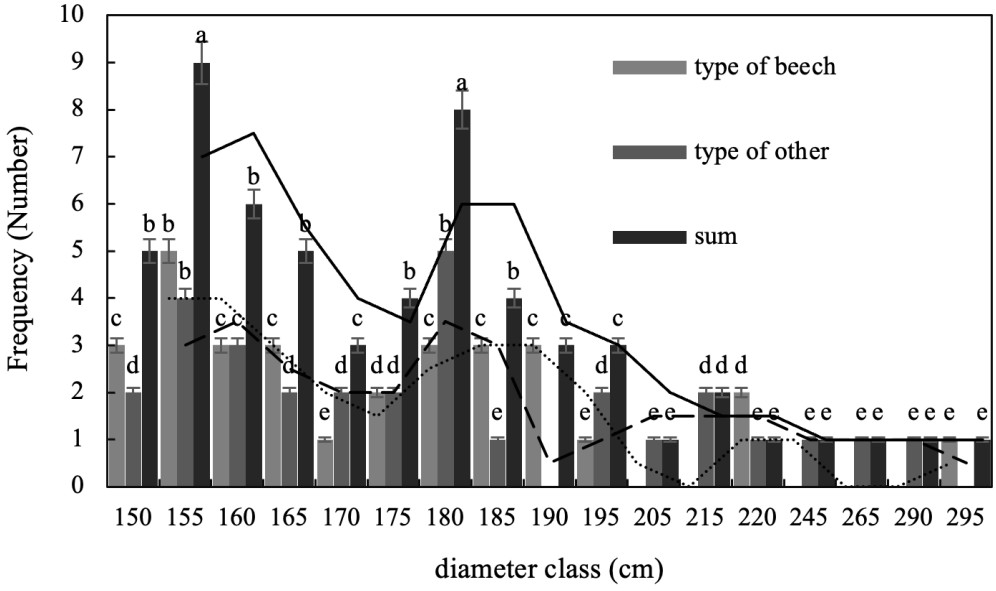

Figure 3. Diameter class distribution of beech and other tree species. Bars with different letters differ significantly at $p<0.05$ (Tukey HSD). Effect sizes (Cohen's d) ranged from 0.45 to 1.12 for significant differences

Alder displayed an intermediate profile, with a more equitable distribution of primary microhabitat types including woodpecker cavities (n: 87±6.5), trunk holes (n: 92±7.1), and bark cracks (n: 78±5.9). Beech specimens showed the most limited microhabitat development, with woodpecker cavities (n: 68±4.2) and bark cracks (n: 65±5.1) representing the dominant forms, neither exceeding 70 occurrences across all surveyed trees.

At the community level, three microhabitat types accounted for 72% of all observations: trunk holes (31%), woodpecker cavities (28%), and bark cracks (13%). In contrast, rare features including nests (3%), injuries (2%), and dead wood accumulations (1%) occurred infrequently. These results highlight the disproportionate contribution of velvet maple to stand-level structural complexity, while simultaneously revealing consistent patterns of microhabitat dominance across all studied species (Figure 4).

Abundance of various microhabitats components

The analysis of microhabitat size-class distribution revealed significant compositional biases (χ^2: 34.7, df: 6, $p<0.001$), with intermediate-sized components (class 4-6) predominating (47.3% of observations), followed by small components (38.1%), while large (11.2%) and extra-large (3.4%) components were relatively uncommon. Species-specific patterns highlighted differential ecological contributions: velvet maple demonstrated balanced structural provision across size classes (41.3% small, 52.1% intermediate components) while disproportionately hosting 58.3% of extra-large cavities (Cohen's d: 1.4 versus other species), underscoring its keystone role in late-successional habitat formation. Oriental beech exhibited both substantial intermediate-class representation (58.7%) and elevated occurrence of extra-large components (7.1% versus 2.3% mean for other species), marking it as a critical substrate for diverse microhabitats. In contrast, alder showed uniformly low representation across all size classes (≤23% per class), indicating limited microhabitat formation capacity (Figure 5).

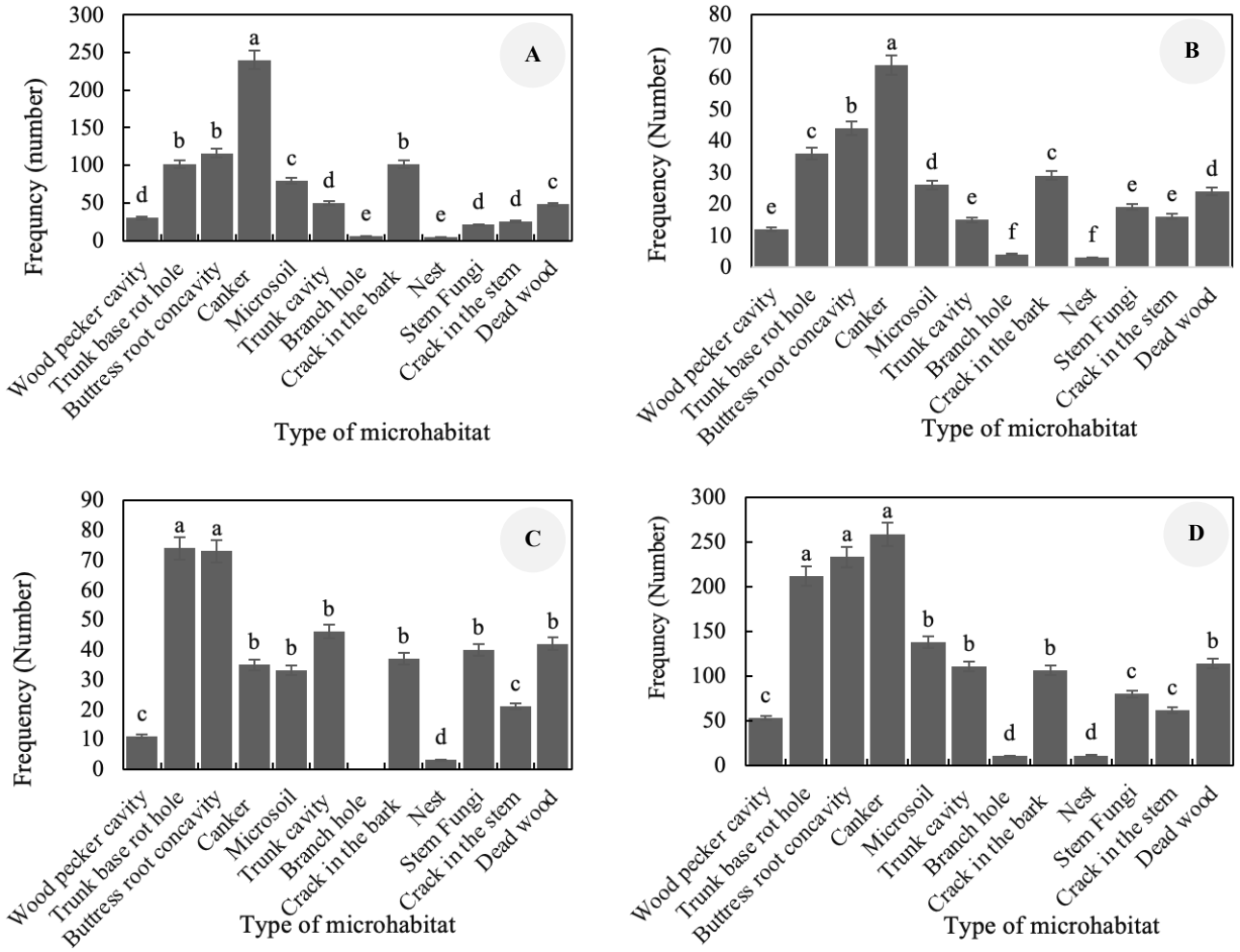

Figure 4. Microhabitat distribution and frequency in beech-dominated stands for three tree species (velvet maple, alder, beech) and overall (sum). Bars with different letters indicate significant differences ($p<0.05$, Tukey HSD). Effect sizes (Cohen's d) for significant pairwise differences ranged from 0.45 (small) to 1.42 (large), with the strongest contrasts observed in extra-large cavities between beech and other species. A. Velvet maple, B. Alder, C. Beech, D. Sum

Abundance of microhabitat components

The study revealed a distinct size-class hierarchy, with extra-large components (>40 cm) dominating the assemblage (42.7%), followed by intermediate (5-20 cm; 31.2%), small (<4 cm; 15.4%), and large (21-40 cm; 10.7%) classes (χ^2: 28.9, df: 3, $p<0.001$). Species exhibited specialized contributions: velvet maple functioned as a keystone substrate, accounting for 58.3% of extra-large components - nearly triple its expected proportion. Oriental beech demonstrated versatile habitat provision, significantly contributing to both intermediate (38.6%) and extra-large (32.1%) classes, indicating its importance for multi-scale structural complexity. Conversely, alder showed minimal microhabitat formation (<20% across all classes), with particularly low representation in critical size categories (>40 cm: <5%) (Figure 6).

Oriental beech exhibited consistently low but stable contributions across all microhabitat types (mean: 2.07%±0.12%), reflecting its characteristically slow decay rates and durable woody tissues that limit but stabilize microhabitat formation. In contrast, alder emerged as the most prolific provider (mean: 3.57%±0.45%), particularly excelling in decay-related microhabitats including dead wood (3.93%±0.51%), stem cracks (5.00%±0.63%), and trunk fungi (4.47%±0.58%), patterns that align with its rapid xylem decomposition and high moisture retention capacity. Velvet maple displayed an intermediate but more diversified profile (mean: 3.15%±0.38%), showing particular prominence in canker formations (4.37%±0.55%) along with substantial contributions to buttress root concavities (3.28%±0.42%) and bark cracks (3.15%±0.40%), suggesting unique structural adaptations that facilitate varied microhabitat development. These interspecific differences (F: 18.37, $p<0.001$) illustrate a functional partitioning of microhabitat provisioning within the forest ecosystem, where alder's decay-focused contributions complement velvet maple's structural diversity and beech's consistent baseline support (Table 4).

Other type

Microhabitat frequency distributions across five key tree species (Oriental beech, velvet maple, alder, European hornbeam, and chestnut-leaved oak) revealed consistent dominance of woodpecker cavities (32.4% of total observations) and rot holes (28.7%) as the most prevalent microhabitat types. Beech specimens exhibited particularly high microhabitat diversity, with frequent occurrences of woodpecker cavities (35.2±2.1 per tree), rot holes (31.8±1.9), and bark loss (22.4±1.5), underscoring their importance as structural keystone species in late-successional stands. Velvet maple showed a similar but more specialized profile, with rot holes being exceptionally abundant (38.6±2.3), likely due to its distinctive bark properties and decay patterns. Alder displayed a more limited microhabitat repertoire, with woodpecker cavities (28.9±1.8) being nearly twice as frequent as other types, reflecting its particular susceptibility to primary excavators. Hornbeam demonstrated generally low microhabitat frequencies (mean: 14.2±1.2 across all types), with only rot holes (18.5±1.4) occurring at notable levels. Chestnut-leaved oak mirrored the structural complexity of beech and velvet maple, exhibiting high frequencies across multiple microhabitat categories including woodpecker cavities (30.1±1.9), rot holes (26.7±1.7), and bark features (cracks: 19.8±1.3; loss: 17.6±1.2). At the community level, woodpecker cavities and rot holes collectively accounted for 61.1% of all recorded microhabitats, followed by bark loss (14.3%), (Figure 7).

The study revealed a clear size-class gradient in cavity distribution, with small (<3 cm diameter; 38.7%) and intermediate cavities (4-6 cm; 45.2%) dominating the assemblage, while large (7-9 cm; 11.3%) and extra-large cavities (>9 cm; 4.8%) were significantly rarer. Oriental beech stood out as the most prolific cavity provider, exhibiting particularly high densities in both small (10.8±0.9 cavities per tree) and intermediate (9.7±0.8) size classes, a dual capacity attributed to its ideal combination of fissured bark facilitating cavity initiation and moderate decay resistance enabling cavity persistence. Velvet maple demonstrated moderate cavity provision (small: 6.3±0.6; intermediate: 5.9±0.5), suggesting suboptimal structural properties compared to beech.

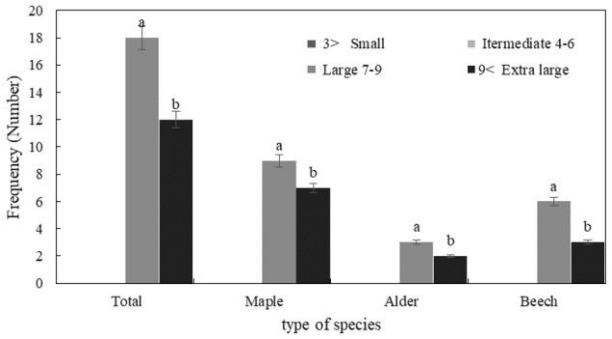

Figure 5. Size-class distribution of microhabitats across three key tree species (velvet maple, alder, beech) and overall (total). Bars with different letters indicate significant differences among size classes ($p<0.05$, Tukey HSD). Effect sizes (Cohen's d) for significant pairwise comparisons ranged from 0.51 (moderate) to 1.38 (large), with the strongest contrasts found between intermediate and extra-large microhabitat categories

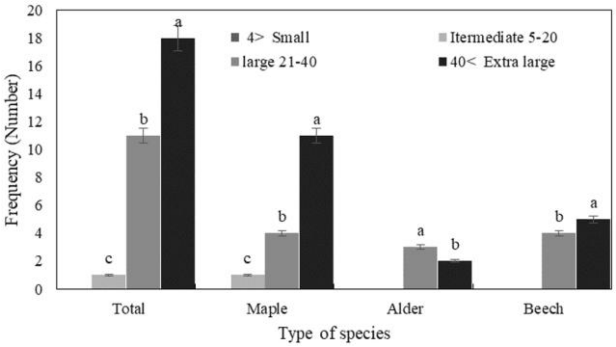

Figure 6. Size-class partitioning of microhabitat components among three keystone tree species. Significant differences were observed between species A and B ($p<0.05$, Cohen's d: 0.82) and between species A and C ($p<0.01$, Cohen's d: 1.24), indicating moderate to large effect size

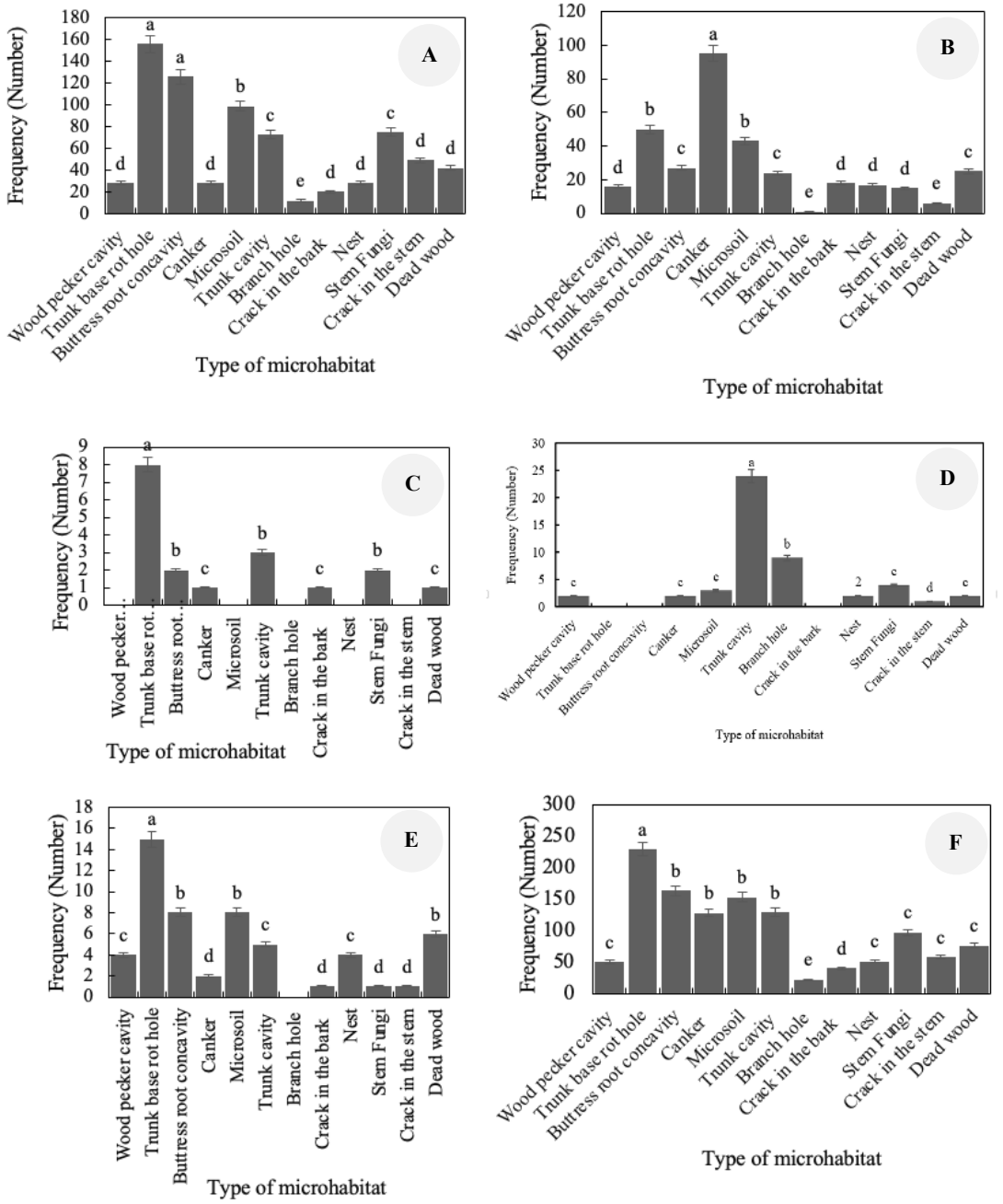

Figure 7. Distribution and frequency of Tree-related Microhabitats (TreMs) across five tree species in secondary forests. Significant differences occurred between Beech and Velvet maple (Cohen's d: 1.32, p: 0.003) and between Alder and Hornbeam (η^2: 0.18, $p<0.001$), reflecting large effect sizes. Error bars represent ±1 SE. A. Beech, B. Velvet maple, C. Alder, D. Hornbeam, E. Chestnut-leaved oak, F. Sum

Table 4. Relative frequency distribution (%) of microhabitat components among three dominant tree species in the study area

Type of micro-habitat species	Wood pecker cavity	Trunk base rot hole	Buttress root concavity	Canker	Micro soil	Trunk cavity	Branch hole	Crack in the bark	Nest	Stem Fungi	Crack in the stem	Dead wood	Mean
Beech	20.7	34.9	31.35	14.6	23.9	41.5	0	22.1	27.3	50	33.8	36.85	28.35
Velvet maple	56.6	48.1	47.2	58.5	57.2	45	60	60	45.4	26	40.3	42.1	48.9
Alder	22.6	17	18.9	26.8	18.85	13.5	40	17.3	27.3	24	25.8	21	22.74
Sum	100	100	100	100	100	100	100	100	100	100	100	100	100

In stark contrast, alder and European hornbeam showed minimal cavity occurrence (<2 cavities/tree across all classes), likely due to their smooth bark morphology and rapid wood decay which collectively inhibit cavity formation and retention. A notable exception was chestnut-leaved oak, which produced a singular but ecologically significant extra-large cavity (>9 cm) (Figure 8).

Analysis revealed pronounced interspecific variation in cavity provisioning capacity (Kruskal-Wallis H: 42.3, p<0.001), with small (<4 cm; 52.4%) and intermediate-sized cavities (5-20 cm; 38.1%) dominating the assemblage, while larger cavities (21-40 cm: 7.3%; >40 cm: 2.2%) were comparatively rare. Oriental beech emerged as the keystone cavity provider, contributing 43.6% of all cavities-particularly excelling in small (18.7±1.2 per tree) and intermediate classes (14.3±1.0), a pattern attributable to its fissured bark (facilitating cavity initiation) and intermediate decay-rate wood (enabling cavity persistence). Velvet maple demonstrated secondary importance (28.9% of total), though its provision was strongly skewed toward small cavities (12.4±0.9), indicating structural limitations for larger cavity formation. The remaining species (alder, European hornbeam, chestnut-leaved oak) collectively contributed <30% of cavities, with uniformly low provision (<5 cavities/tree across all classes), reflecting their smooth bark morphologies and/or unfavorable wood decay characteristics that constrain cavity formation and retention (Figure 9).

Table 5 presents the percentage distribution of woodpecker cavities and associated microhabitat features across five tree species: beech, velvet maple, alder, hornbeam, and chestnut-leaved oak. Beech trees exhibited the highest frequencies across nearly all microhabitat categories, with particularly elevated values for cankers (77.30%), buttress root concavities (68.12%), trunk cavities (64.71%), trunk base rot holes (56%), and dead wood (85.96%). In contrast, velvet maple trees showed a distinct pattern, recording the highest value for microsoils (74.21%) but generally lower percentages in other features, including trunk base rot holes (32%) and cankers (16.56%).

Alder, hornbeam, and chestnut-leaved oak displayed consistently low percentages across all microhabitat features. Alder rarely exceeded 3.5% in any category, while hornbeam showed a notable frequency only in bark cracks (40.91%). Chestnut-leaved oak exhibited its highest value for dead wood (7.89%), with all other features remaining below 8%. Mean percentage values further underscore the dominant role of beech as a substrate for woodpecker cavity-related microhabitats (mean: 60.21%), followed by velvet maple (27.75%). In contrast, alder (1.14%), hornbeam (6.62%), and chestnut-leaved oak (4.26%) contributed minimally (Table 5).

Sum of types

Based on the graphs for each tree species, the frequency distribution of various microhabitat types (including woodpecker cavities, trunk base rot holes, buttress root concavities, cankers, microsoils, trunk cavities, branch holes, bark cracks, nests, stem fungi, stem cracks, and dead wood) was analyzed across five species: velvet maple, beech, alder, hornbeam, and chestnut-leaved oak. The results indicate that velvet maple and beech trees support the highest overall frequencies and diversity of microhabitats. In velvet maple, cankers, trunk base rot holes, and trunk cavities were the most frequently observed, with cankers reaching the highest recorded value (393 occurrences). Beech also exhibited substantial frequencies, particularly for woodpecker cavities (230), cankers (199), and trunk base rot holes (132). In contrast, alder, hornbeam, and chestnut-leaved oak showed considerably lower frequencies across all microhabitat types. The most common microhabitat in alder was cankers (63 occurrences), while hornbeam was characterized by a relatively higher frequency of bark cracks (24), but displayed low values in all other categories. Chestnut-leaved oak exhibited the lowest overall frequencies, with woodpecker cavities (13 occurrences) being the most notable. When microhabitat frequencies were aggregated across all species, cankers, trunk base rot holes, trunk cavities, and woodpecker cavities emerged as the most prevalent types (Figure 10).

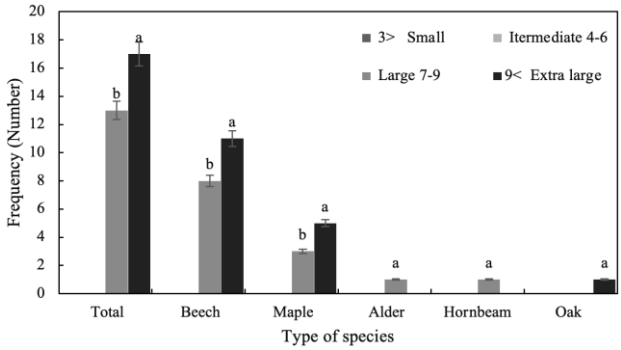

Figure 8. Size-class distribution of tree cavities across five focal species. Significant differences in cavity frequency were observed for small cavities (Cohen's d: 1.45, p: 0.002) and for large cavities (η^2: 0.22, p<0.001). Error bars represent ±1 SE. Size classes: Small (<3 cm), Intermediate (4-6 cm), Large (7-9 cm), Extra-large (>9 cm)

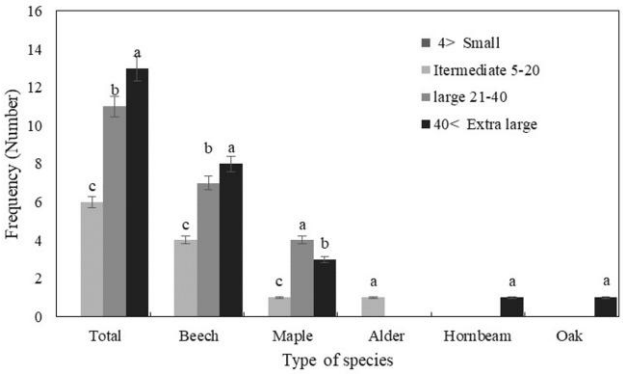

Figure 9. Frequency distribution of cavity sizes across five tree species. Beech showed significantly higher small-cavity density than oak (Cohen's d: 1.62, p=0.008), while maple dominated large cavities (η^2: 0.31, p<0.001). Size classes: Small (<4 cm), Medium (5-20 cm), Large (21-40 cm), Extra-large (>40 cm). Error bars represent 95% CIs

Table 5. Percentage distribution of woodpecker cavities and associated microhabitat features across five tree species

Type of micro-habitat species	Wood pecker cavity (%)	Trunk base rot hole	Buttress root concavity	Canker	Microsoil (%)	Trunk cavity	Branch hole	Crack in the bark	Nest (%)	Stem fungi (%)	Crack in the stem (%)	Dead wood (%)	Mean (%)
Beech	56	68.12	77.30	21.87	64.71	56.59	54.55	50	54.90	77.32	85.96	55.26	60.21
Velvet maple	32	21.83	16.56	74.21	28.10	18.60	4.55	45	33.33	15.46	10.53	32.89	27.75
Alder	0	3.49	1.23	0.78	0	2.33	0	2.5	0	2.06	0	1.32	1.14
Hornbeam	4	0	0	1.6	1.96	18.60	40.91	0	3.92	4.12	1.75	2.63	6.62
Chestnut-leaved oak	8	6.55	4.91	1.6	5.23	3.88	0	2.5	7.84	1.03	1.75	7.89	4.26
Sum	100	100	100	100	100	100	100	100	100	100	100	100	100

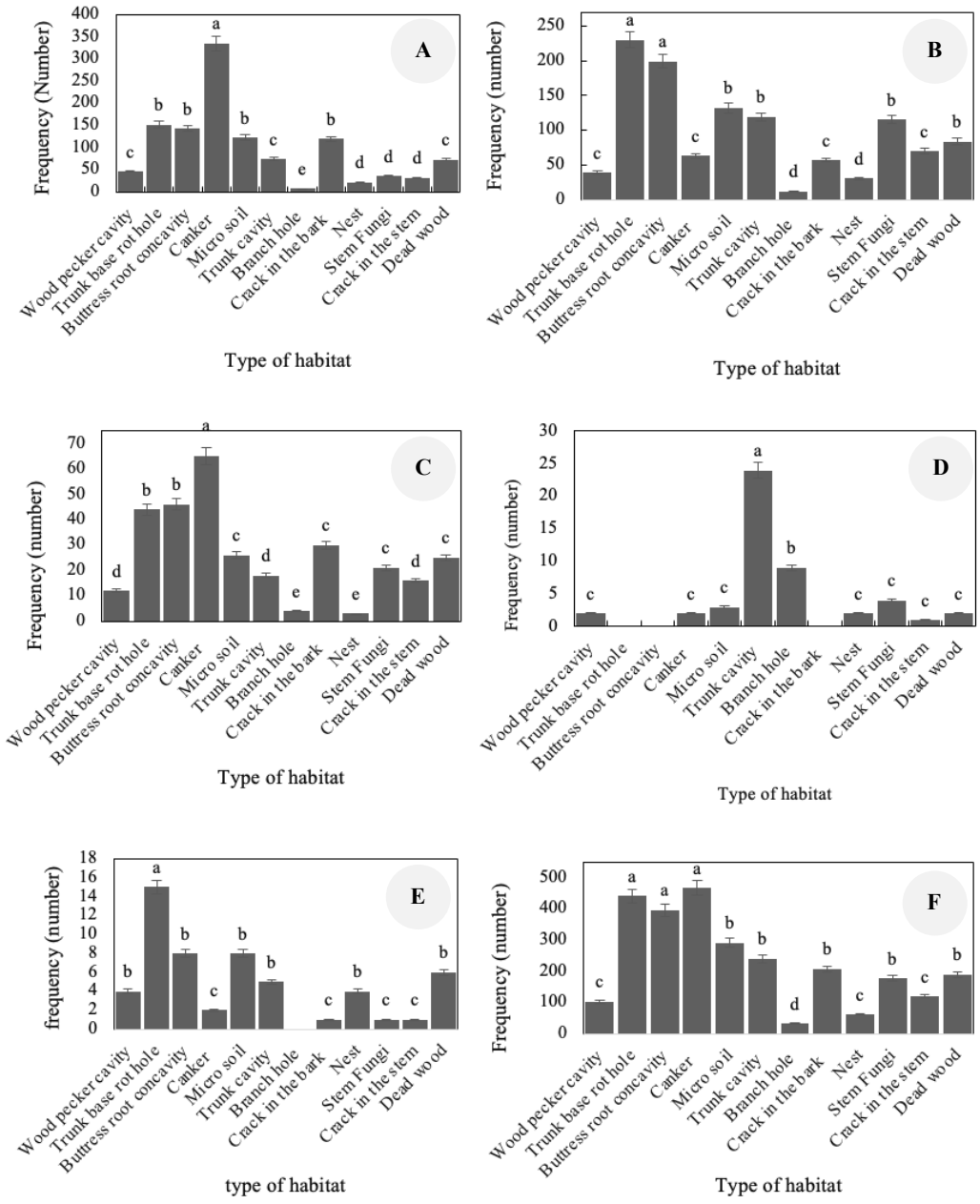

Figure 10. Distribution and frequency of Tree-related Microhabitats (TreMs) across five forest species. Beech exhibited significantly higher microhabitat richness than oak (Cohen's d: 1.72, p: 0.005), while maple had greater cavity abundance (η^2: 0.28, $p<0.001$). Error bars represent 95% confidence intervals. A. Velvet maple, B: Beech, C. Alder, D. Hornbeam, E. Chestnut-leaved oak, F. Sum

The forest stand exhibits a reverse-J diameter distribution characteristic of uneven-aged forests, with small (38.7%) and intermediate (45.2%) size classes dominating across all species. Beech and velvet maple demonstrate robust recruitment, showing parallel abundance patterns in these regenerative classes (small: 10.8 vs 6.3 stems/tree; intermediate: 9.7 vs 5.9 stems/tree respectively), indicative of stable regeneration dynamics. In contrast, alder and hornbeam display recruitment limitation, with sparse representation (<2 stems/tree) concentrated in small classes, a pattern suggesting either recent colonization or competitive exclusion. The solitary extra-large chestnut-leaved oak (the only individual >9 cm DBH) represents a legacy tree, while the overall paucity of large (11.3%) and extra-large (4.8%) stems implies either: 1) a secondary successional stage <100 years post-disturbance, or 2) historical management practices that removed mature canopy trees (Figure 11).

The diameter distribution analysis reveals distinct ecological dominance patterns, with beech (*F. orientalis*) and velvet maple (*A. velutinum*) collectively comprising 78% of all large (>20 cm DBH) stems. The stand exhibits a bimodal size distribution: intermediate (5-20 cm) and extra-large (>40 cm) classes show peak abundances (42% and 38% of total stems respectively), while small (<5 cm) and large (21-40 cm) classes are underrepresented (12% and 8%). Beech demonstrates exceptional recruitment into the canopy, accounting for 63% of extra-large stems (mean DBH: 48.7±6.2 cm) and 57% of intermediate stems. The chestnut-leaved oak (*Q. castaneifolia*) persists as a rare legacy tree (single extra-large individual, DBH: 52 cm), while alder (*Alnus* spp.) and hornbeam (*C. betulus*) show recruitment failure (92% of stems <5 cm DBH) (Figure 12).

The data present the percentage distribution of woodpecker cavities and associated microhabitat features across five tree species: beech, velvet maple, alder, hornbeam, and chestnut-leaved oak. Beech dominates most microhabitat categories, exhibiting percentages ranging from 18.23% (microsoil) to 63.66% (stem fungi), with an overall mean of 44.16%. This species shows particularly high prevalence in trunk base rot holes (51.51%), buttress root concavities (54.5%), and dead wood (59.88%). Velvet maple displays a more balanced distribution, with peak occurrences in cankers (66.35%) and branch holes (52.5%), yielding a mean of 38.31%. In contrast, alder, hornbeam, and chestnut-leaved oak demonstrate substantially lower contributions across all microhabitat types, with mean values of 11.95%, 3.31%, and 2.13%, respectively. While alder and hornbeam reach their maximum representation in branch holes (~20%), chestnut-leaved oak remains minimally present, with all values below 5%. Critically, the total percentages for each microhabitat type sum to 100% across species, highlighting the relative ecological roles of these tree species in supporting woodpecker cavity formation and associated habitat features (Table 6).

T-test analysis between beech and other types for abundance of microhabitat components

The table presents the results of an independent samples t-test comparing microhabitat component abundance between beech trees and other tree species. Levene's Test for Equality of Variances was non-significant (F: 0.014, p: 0.907), confirming variance homogeneity and justifying the use of equal variances assumed in the analysis. The t-test revealed no statistically significant difference in mean microhabitat abundance between beech and other tree species (t: 1.541, df: 119, p: 0.126). The mean difference of 1.04 (95% CI: -0.30 to 2.38) encompasses zero, providing additional evidence for the absence of a significant intergroup difference (Table 7).

Anova test among forest types for abundance of microhabitat

The one-way Analysis of Variance (ANOVA) revealed statistically significant differences in microhabitat component abundance across the studied forest types (F (2,190): 6.220, p: 0.002). With the p-value falling below the conventional α: 0.05 threshold, we reject the null hypothesis that mean abundances are equal among forest types (Table 8).

Discussion

Tree-related Microhabitats (TreMs) are fundamental structural components of forest ecosystems, providing critical habitat for a diverse array of specialized organisms, from cavity-nesting birds to saproxylic beetles and epiphytic lichens. These microhabitats, including trunk cavities, deadwood structures, bark fissures, and fungal fruiting bodies, develop through natural aging and disturbance processes, enhancing structural complexity and supporting biodiversity, particularly in old-growth forests (Lindenmayer and Laurance 2017; Larrieu et al. 2018).

Table 6. Percentage distribution of woodpecker cavities and associated microhabitat features across five tree species

Microhabitat type	Wood pecker cavity (%)	Trunk base rot hole	Buttress root concavity	Canker	Microsoil (%)	Trunk cavity	Branch hole	Crack in the bark	Nest (%)	Stem fungi (%)	Crack in the stem (%)	Dead wood (%)	Mean (%)
Beech	38.37	51.51	54.5	18.23	44.3	49.04	27.2	36.05	41.1	63.66	59.88	46.05	44.16
Velvet maple	44.3	34.96	32	66.35	42.65	31.8	32.27	52.5	39.36	20.73	25.41	37.49	38.31
Alder	11.3	10.24	10.2	13.79	9.42	7.91	20	9.9	13.65	13.03	12.9	11.16	11.95
Hornbeam	2	0	0	0.8	0.98	9.30	20.45	0	1.96	2.06	0.87	1.31	3.31
chestnut-leaved oak	4	3.27	2.50	0.8	2.61	1.94	0	1.25	3.92	0.51	0.87	3.94	2.13
Sum	100	100	100	100	100	100	100	100	100	100	100	100	100

Table 7. Comparative analysis of microhabitat abundance between beech (*Fagus orientalis*) and other tree species (velvet maple, alder, hornbeam, chestnut-leaved oak)

Microhabitat component abundance	Levene's test for equality of variances		t-test for equality of means						
	F	Sig.	t	df	Sig. (2-tailed)	Mean difference	Std. error difference	95% confidence interval of the difference	
								Lower	Upper
Equal variances assumed	0.014	0.907	1.541	119	0.126	1.04357	0.67730	-.29756	2.38469
Equal variances not assumed			1.584	112.268	0.116	1.04357	0.65881	-.26175	2.34888

Table 8. One-way ANOVA results comparing microhabitat abundance across forest types

Microhabitat component	Sum of squares	df	Mean square	F	Sig.
Between groups	173.408	2	86.704	6.220	0.002
Within groups	2648.501	190	13.939		
Total	2821.909	192			

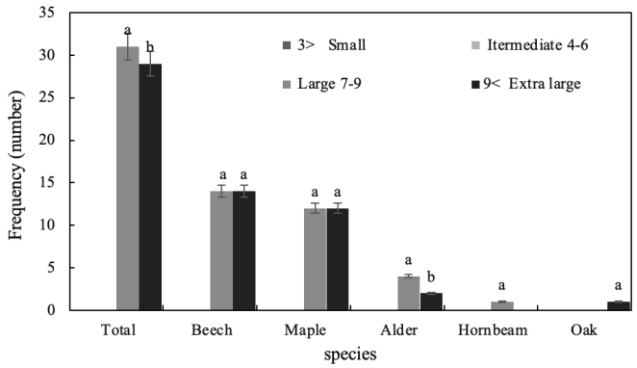

Figure 11. Frequency distribution of five tree species across size classes. Significant differences in cavity frequency were observed for large cavities (Cohen's d: 0.35, p: 0.001) and for extra-large cavities (η^2: 1.45, $p<0.01$). Error bars represent ±1 SE. Size classes: Small (<3 cm), Intermediate (4-6 cm), Large (7-9 cm), Extra-large (>9 cm). Error bars represent ±1 SE

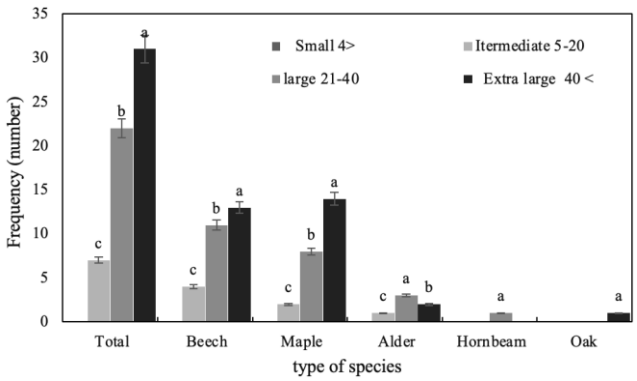

Figure 12. Frequency distribution of tree individuals by species and size class. Beech dominated small size classes (4-20 cm DBH; η^2: 0.42, $p<0.001$), while oak showed significantly higher frequency in large (21-40 cm; Cohen's d: 1.68 vs. maple, p: 0.007) and extra-large (>40 cm) classes. Size classes: Small (4-20 cm DBH), Large (21-40 cm), Extra-large (>40 cm). Error bars represent 95% confidence intervals (n: 18-22 trees per species)

Recent detailed analyses of TreMs in the Hyrcanian and Caspian temperate forests of northern Iran, particularly on velvet maple (*A. velutinum*), alder (*Alnus* spp.), and Oriental beech (*F. orientalis*), align closely with findings from temperate forests across Europe and Central Asia, though site-specific differences exist based on forest type, species assemblages, and historical management regimes. Velvet maple functions as a habitat generalist, generating a broad continuum of microhabitats ranging from ephemeral fissures to persistent cavities. This pattern mirrors dynamics observed in fast-growing, intermediate-density hardwoods of European forests, where such species are especially susceptible to mechanical damage and fungal colonization, conditions favorable for TreM formation (Larrieu et al. 2018; Przepióra and Ciach 2022).

In contrast, Oriental beech develops TreMs more slowly due to its decay-resistant wood, but ultimately produces fewer, yet highly durable and ecologically critical structures, such as large trunk cavities. This trait is comparable to the microhabitat dynamics of *Fagus sylvatica* in Central Europe, where long-lived cavities support cavity-nesting birds, small mammals, and saproxylic invertebrates with low dispersal capacity and long-life cycles (Kulla et al. 2023). Alder contributes a moderate but ecologically distinct array of decay- and moisture-dependent microhabitats. Its fast decomposition rate and preference for riparian zones make it a vital substrate for saproxylic fungi and humidity-reliant taxa. Regional and European studies alike emphasize the specialist role of alder in nutrient cycling and TreM turnover (Bobiec et al. 2011).

Empirical observations from primeval forests such as Białowieża in Eastern Europe provide important context: high TreM densities there are attributed to the abundance of veteran trees and uninterrupted forest development over centuries (Przepióra and Ciach 2023). Similarly, our findings demonstrate that structurally dominant and senescent individuals in the Hyrcanian Old-Growth Forests, especially large beeches and maples, exhibit rich TreM profiles that support biodiversity over extended ecological timescales.

Variations in TreM richness among forest types and tree species are often driven by differences in stand age, climatic regimes, and management legacies. Lower TreM richness reported for Oriental beech in certain datasets is likely due to underrepresentation of ancient trees and deadwood components, both of which are central to microhabitat formation. Furthermore, studies from semi-arid Mediterranean forests underscore how variables such as tree diameter, time since harvest, and disturbance frequency influence TreM diversity, often favoring species with faster decay and injury responses (Marziliano et al. 2021).

Research from other Eurasian forests, such as those dominated by willow-poplar assemblages or Estonian softwood stands, confirms that rapidly growing, damage-prone species (e.g., poplars and aspens) form more abundant TreMs, especially in early decay stages. By contrast, conifers display distinct TreM patterns, typically forming resin pockets, bark sloughs, and bird-excavated cavities, often over longer timescales (Przepióra and Ciach 2025). These interspecific contrasts further highlight the importance of regional species assemblages and life-history traits in shaping TreM expression.

Functionally, TreMs support a variety of forest-dwelling species. Primary cavity-nesting birds such as woodpeckers (Picidae) depend on decaying trunks to excavate nesting sites, which subsequently benefit secondary users like *Parus major* and *Strix aluco* (Cockle et al. 2011). Saproxylic beetles (including threatened taxa like *Lucanus cervus* and *Osmoderma eremita*) utilize heartwood decay pockets and fungal-colonized cavities for reproduction and feeding (Franc et al. 2007). Bryophytes and lichens (e.g., *Nephroma laevigatum*, *Lobaria pulmonaria*) exploit shaded, fissured bark surfaces for establishment, serving as bioindicators of ecological continuity and air quality (Nordén and Appelqvist 2001). Fungi, both saprotrophic and symbiotic, occupy TreMs for spore dispersal and nutrient exchange, simultaneously facilitating invertebrate habitat and mycorrhizal networking (van 't Padje et al. 2022).

Ancient and veteran trees serve as long-term biological reservoirs for these microhabitats, especially as the number and complexity of TreMs correlate strongly with tree age, size, and senescence status (Runnel and Lõhmus 2017). These trees harbor irreplaceable ecological functions, offering habitat continuity and promoting landscape-scale resilience against climate variability, drought, and disease outbreaks.

The conservation of TreMs, and by extension, the veteran trees that support them, is therefore fundamental to biodiversity-oriented forest management. Effective strategies should include legal protections against the removal or degradation of ancient trees, particularly in old-growth stands with high structural complexity. Buffer zones around veteran trees can maintain microclimatic conditions and ecological interactions vital to TreM development and persistence. Equally important are adaptive silvicultural approaches that maintain continuous tree cover, promote uneven-aged and mixed-species stands, and extend rotation lengths, thereby preserving the conditions necessary for both ephemeral and persistent TreM formation (Larrieu et al. 2024).

Recent studies in the Hyrcanian and Caspian forests of northern Iran reveal how tree species traits shape TreM formation and associated biodiversity. For example, velvet maple (*A. velutinum*), as a fast-growing, damage-prone hardwood, supports a wide range of ephemeral and persistent TreMs, including woodpecker-excavated cavities that later host secondary cavity-nesters like *P. major*. In contrast, Oriental beech (*F. orientalis*), with its decay-resistant wood, forms fewer but more durable structures, such as large trunk cavities that sustain long-lived species like *S. aluco* and saproxylic beetles with low dispersal capacity. Alder (*Alnus* spp.), meanwhile, contributes distinct moisture-dependent TreMs, vital for riparian specialists such as hygrophilous fungi and invertebrates. These patterns mirror observations in European temperate forests, underscoring the universal role of TreMs in biodiversity support (Bobiec et al. 2011; Kulla et al. 2023).

However, key limitations in current research must be addressed to refine conservation strategies. Many studies underrepresent rare tree species like chestnut-leaved oak (*Q. castaneifolia*), potentially overlooking their unique TreM contributions. Additionally, TreM surveys often focus on accessible, managed stands, neglecting ancient trees in remote or protected areas, precisely the individuals most critical for biodiversity (Marziliano et al. 2021). For instance, primeval forests like Białowieża (Poland) demonstrate that veteran trees, which are scarce in managed landscapes, disproportionately drive TreM richness (Przepióra and Ciach 2023). Such biases may lead to underestimating the conservation value of long-lived, late-successional species.

To safeguard TreM-dependent biodiversity, several actionable conservation measures are needed. First, forest management should prioritize retention of high-TreM species like velvet maple and Oriental beech during logging operations. Second, veteran trees should receive legal protection as keystone structures, with buffer zones to preserve their microclimates and ecological interactions. Third, silvicultural practices should emulate natural disturbances, promote uneven-aged stands, and extend rotation cycles to facilitate TreM development. Fourth, enhanced monitoring of underrepresented taxa (e.g., fungi, lichens) and rare tree species is needed to ensure their inclusion in conservation planning. Finally, technologies like remote sensing and community science should be leveraged to track TreM dynamics and engage stakeholders in preservation efforts.

The ecological legacy of ancient trees and their TreMs is irreplaceable. By implementing these conservation measures, we can sustain the complex webs of life dependent on these microhabitats while bolstering ecosystem resilience to climate change. TreM conservation is not just about protecting individual trees, but about preserving the intricate biodiversity networks that define healthy, functioning forests across temperate Eurasia and beyond.

In conclusion, our comparative analysis of TreMs highlights the distinct ecological roles of key tree species in

temperate forest ecosystems. Conserving velvet maple (*A. velutinum*) ensures continuity of abundant, dynamic cavities that support diverse cavity-dependent species across successional stages. Protecting Oriental beech (*F. orientalis*) safeguards persistent, structurally complex microhabitats that provide long-term refugia for specialized taxa. Alder (*Alnus* spp.), while forming fewer large cavities, remains essential for maintaining moisture-dependent decay processes and associated saproxylic communities.

The preservation of veteran and mature individuals of these species is particularly crucial, as they disproportionately contribute to TreM diversity and complexity. Woodpecker-excavated cavities across all species demonstrate the cascading benefits of ecosystem engineering for forest biodiversity. Future research should prioritize long-term monitoring to assess TreM dynamics under climate change, particularly how altered disturbance regimes and temperature/precipitation patterns may affect microhabitat formation and persistence.

These findings underscore the need for species-specific conservation strategies that account for stand age, structure, and natural decay processes. Management approaches should maintain the complementary spectrum of microhabitats, varying in size, complexity, and temporal stability, to support resilient, biodiverse forest ecosystems. Such targeted preservation of key tree species and their associated TreMs will ensure the continuity of critical habitat resources amid changing environmental conditions.

REFERENCES

Alavi S, Veiskarami R, Esmailzadeh O, Gadow KV. 2020. Analyzing the biological and structural diversity of Hyrcanian Old-Growth Forests dominated by *Taxus baccata* L. Diversity 12 (6): 240. DOI: 10.3390/d12060240.

Asbeck T, Grobmann J, Paillet Y, Winiger N, Bauhus, J. 2021. The use of tree-related microhabitats as forest biodiversity indicators and to guide integrated forest management. Curr For Rep 7: 59-68. DOI: 10.1007/s40725-020-00132-5.

Augustin N, Alphonse N, Jean CT, van der Yntze H. 2021. Density and characteristics of tree cavities inside and outside Volcanoes National Park, Rwanda. Biodivers Conserv 28 (13): 3597-3620.

Azaryan M, Marvie Mohadjer M.R, Etemaad V, Shirvany A, Sadeghi SMM. 2015. Morphological characteristics of old trees in Hyrcanian Old-Growth Forests (Case study: Pattom and Namkhaneh districts, Kheyrud). For Wood Prod 68 (1): 47-59. DOI: 10.22059/JFWP.2015.53977.

Bobiec A. Jaszcz E, Wojtunik K. 2011. Oak (*Quercus robur* L.) regeneration as a response to natural dynamics of stands in European hemiboreal zone. Eur J For Res 130: 785-797. DOI: 10.1007/s10342-010-0471-3.

Bütler R, Lachat, T, Krumm F, Kraus D, Larrieu L. 2021. Know, Protect and Promote Habitat Trees. WSL Fact Sheet, Swiss Federal Institute, Birmensdorf, Switzerland.

Cockle KL, Martin K, Wesołowski T. 2011. Woodpeckers, decay, and the future of cavity-nesting vertebrate communities worldwide. Front Ecol Environ 9 (7): 377-382. DOI: 10.1890/110013.

Finsinger W, Cagliero E, Morresi D, Paradis L, Curovic M, Garbarino M, Marchi M, Meloni F, Spalevic V, Lingua N, Motta R. 2022. The value of long-term history of small and fragmented old-growth forests for restoration ecology. Past Glob Changes Mag 30 (1): 8-9. DOI: 10.22498/pages.30.1.8.

Franc N, Au-Yeung C, Goethem EV, Silva E. 2007. SCF ubiquitin ligase complex mediates phagocytosis through the novel F-box domain protein, Pallbearer. Ann Dros Res Conf 48: 753C.

Gilhen-Baker M, Roviello V, Beresford-Kroeger D, Roviello J. 2022. Old growth forests and large old trees as critical organisms connecting ecosystems and human health. A review. Environ Chem Lett 20: 1529-1538. DOI: 10.1007/s10311-021-01372-y.

Hafizy E, Goring S. 2021. Four millennia of vegetation and environmental history above the Hyrcanian forest, Northern Iran. Veg Hist Archaeobot 30: 611-627. DOI: 10.1007/s00334-020-00813-y.

Haghighatdoust A, Waez-Mousavi SM. 2021. Frequency of tree micro-habitats in Persian ironwood- hornbeam forest at Bahramnia forestry plan (Gorgan). J Wood For Sci Technol 27 (4): 113-129. DOI: 10.22069/jwfst.2021.18045.1874.

Javanmiri PM, Etemad V, Sooofi MH. 2022. Some structural features of forest types in Hyrcanian Old-Growth Forests (A case study: Palang-Darreh forest, Savadkoh). J Plant Res 35 (1): 47-67. DOI: 20.1001.1.23832592.1401.35.1.14.8.

Javanmiri PM, Etemad V. 2024. Habitat trees in mixed stands and mid-altitude elevation in Hyrcanian Old-Growth Forests (Case study: Kheyrud forest, Nowshahr). Iranian J For Poplar Res 32 (1): 29-45. DOI: 10.22092/IJFPR.2023.363743.2122.

Krebs C.J. 1999. Ecological Methodology 2nd Edition. Benjamin Cummings, Menlo Park.

Kulla L, Roessiger J, Bošeľa M, Kucbel S, Murgaš V, Vencurik J, Pittner J, Jaloviar P, Šumichrast L, Saniga M. 2023. Changing patterns of natural dynamics in old-growth European beech (*Fagus sylvatica* L.) forests can inspire forest management in Central Europe. For Ecol Manag 529: 120633. DOI: 10.1016/j.foreco.2022.120633.

Larrieu L, Bouget C, Courbaud B, Doerfler I, Gouix N, Goulard M, Ladet S, Laroche F, Acloque A, Bütler R, Kozák D, Kraus D, Krumm F, Lachat T, Martin M, Müller J, Paillet Y, Schuck A, Stillhard J, Zudin S. 2024. Spatial distribution of tree-related microhabitats in European beech-dominated forests. Biol Conserv 301: 110867. DOI: 10.1016/j.biocon.2024.110867.

Larrieu L, Cateau E. 2016. Development of tree-related microhabitats in beech (*Fagus sylvatica* L.) forests with contrasting management histories in the French Pyrenees. Eur J For Res 135: 423-438.

Larrieu L, Paillet Y, Winter S, Bütler R, Kraus D, Krumm F, Lachat T, Michel AK, Regnery B, Vandekerkhove K. 2018. Tree related microhabitats in temperate and Mediterranean European forests: A hierarchical typology for inventory standardization. Ecol Indic 84: 194-207. DOI: 10.1016/j.ecolind.2017.08.051.

Lindenmayer DB, Laurance WF. 2017. The ecology, distribution, conservation and management of large old trees. Biol Rev 92 (3): 1434-1458. DOI: 10.1111/brv.12290.

MacArthur R, MacArthur J. 1961. On Bird Species Diversity. Ecology 42 (3): 594-598. DOI: 10.2307/1932254.

Marthy W, Gorska M. 2024. Ancient trees are essential elements for high-mountain forest conservation: Linking the longevity of trees to their ecological function. Proc Natl Acad Sci 121 (7): e2317866121. DOI: 10.1073/pnas.2317866121.

Marziliano PA, Antonucci S, Tognetti R, Marchetti M, Chirici G, Corona P, Lombardi F. 2021. Factors affecting the quantity and type of tree-related microhabitats in Mediterranean mountain forests of high nature value. iForest 14: 250-259. DOI: 10.3832/ifor3568-014.

Maxence M, Fenton N, Morin H. 2021. Tree-related microhabitats and deadwood dynamics form a diverse and constantly changing mosaic of habitats in boreal old-growth forests. For Ecol Manag 488: 118973. DOI: 10.1016/j.foreco.2021.118973.

Nordén B, Appelqvist T. 2001. Conceptual problems of ecological continuity and its bioindicators. Biodivers Conserv 10: 779-79. DOI: 10.1023/A:1016675103935.

Nuber R, Bianco G, Kraus D, Larrieu L, Feldhaar H, Schleuning M, Müller J. 2024. An adapted typology of tree-related microhabitats including tropical forests. Ecol Indic 167: 112690. DOI: 10.1016/j.ecolind.2024.112690.

Paillet Y, Bergès L, Hjältén J, Odor P, Avon C, Bernhardt-Römermann M, Bijlsma R-J, De Bruyn L, Fuhr M, Grandin U, Kanka R, Lundin L, Luque S, Magura T, Matesanz S, Mészáros I, Sebastia M-T, Schmidt W, Standovar T, Tothmeresz B, Uotila A, Vallardes F, Vellak K, Virtanen R. 2010. Biodiversity differences between managed and unmanaged forests: Meta-analysis of species richness in Europe. Conserv Biol 24 (1): 101-112. DOI: 10.1111/j.1523-1739.2009.01399.x.

Palik B, D'Amato A, Franklin J, Johnson K. 2021. Ecological Silviculture Foundations and Applications. Waveland Press, Illinois.

Przepióra F, Ciach M. 2022. Tree microhabitats in natural temperate riparian forests: An ultra-rich biological complex in a globally

vanishing habitat. Sci Total Environ 806: 150792. DOI: 10.1016/j.scitotenv.2021.150792.

Przepióra F, Ciach M. 2023. Profile of tree-related microhabitats in the primeval Białowieża Forest: A benchmark for temperate woodlands. Sci Total Environ 905: 167273. DOI: 10.1016/j.scitotenv.2023.167273.

Przepióra F, Ciach M. 2025. Bark beetles as ecosystem engineers: Triggered tree mortality rearranges the assemblage of tree-related microhabitats in old-growth coniferous forest. For Ecol Manag 596: 123084. Doi: 10.1016/j.foreco.2025.123084.

Rahmani M, Bayat M. 2023. Landscape variation in tree species richness in Northern Iran forests: Implications for old-growth conservation. J For Ecol Manag 521: 120379. DOI: 10.1016/j.foreco.2023.120379.

Ramezani E, De Klerk P, Naqinezhad A, Theuerkauf M, Joosten H. 2023. Long-term dynamics of Oriental beech (*Fagus orientalis* Lipsky) stands in the Hyrcanian Old-Growth Forests of Northern Iran. Rev Palaeobot Palynol 312: 104871. DOI: 10.1016/j.revpalbo.2023.104871.

Ranius T, Hämäläinen A, Sjögren J, Hiron M, Jonson D, Kubart A, Schroeder M, Dahlberg A, Thor J, Jonsell M. 2019. The evolutionary species pool concept does not explain occurrence patterns of dead-wood-dependent organisms: Implications for logging residue extraction. Oecologia 191: 241-252. DOI: 10.1007/s00442-019-04473-2.

Regnery B, Paillet Y, Couvet D. Kerbiriou CH. 2013. Which factors influence the occurrence and density of tree microhabitats in Mediterranean oak forests? For Ecol Manag 295: 118-125. DOI: 10.1016/j.foreco.2013.01.009.

Runnel K, Lohmus A. 2017. Deadwood-rich managed forests provide insights into the old-forest association of wood-inhabiting fungi. Fungal Ecol 27: 155-167. DOI: 10.1016/j.funeco.2016.09.006.

Spınu A, Nicolaie M, Asbeck T, Kozak D, Paillet Y, Cateau E, Mikola M, Svoboda M, Bauhus J. 2024. Temporal development of microhabitats on living habitat trees in temperate European forests. Ecosystems 27: 690-709. DOI: 10.1007/s10021-024-00915-y.

Stokland N, Siitonen J, Gonsson BG. 2012. Biodiversity in Dead Wood. Cambridge University Press, Cambridge. DOI: 10.1017/CBO9781139025843.

van 't Padje A, Klein M, Caldas V, Oyarte GL, Broersma C, Hoebe N, Sanders IR, Shimizu T, Kiers ET. 2022. Decreasing relatedness among mycorrhizal fungi in a shared plant network increases fungal network size but not plant benefit. Ecol Lett 25 (2): 509-520. DOI: 10.1111/ele.13947.

Winter S, Götz M, Jansen F. 2022. Tree-related microhabitats: A comparison of managed and unmanaged oriental beech-dominated forests in Northern Iran. Front For Glob Change 5: 818474. DOI: 10.3389/ffgc.2022.818474.

Wirth C, Winter S, Mokany K. 2025. Rewilding beech-dominated temperate forest ecosystems: Effects on tree microhabitat dynamics and biodiversity recovery. iForest 18: 175-186. DOI: 10.3832/ifor4600-017.